SAND2022-3901C

22PFL-0474

A Review of Current Understanding of the Underlying Physics Governing the Interaction, Ignition and Combustion Dynamics of Multiple-injections in Diesel Engines

Author, co-author (Do NOT enter this information. It will be pulled from participant tab in MyTechZone)

Affiliation (Do NOT enter this information. It will be pulled from participant tab in MyTechZone)

Abstract

This work is a comprehensive technical review of existing literature and a synthesis of current understanding of the governing physics behind the interaction of multiple fuel injections, ignition, and combustion behavior of multiple-injections in diesel engines. Multiple-injection is a widely adopted operating strategy applied in modern compression-ignition engines, which involves various combinations of small pre-injections and post-injections of fuel before and after the main injection and splitting the main injection into multiple smaller injections. This strategy has been conclusively shown to improve fuel economy in diesel engines while achieving simultaneous NO_X, soot, and combustion noise reduction – in addition to a reduction in the emissions of unburned hydrocarbons (UHC) and CO by preventing fuel wetting and flame quenching at the piston wall. Despite the widespread adoption and an extensive literature documenting the effects of multiple-injection strategies in engines, little is known about the complex interplay between the underlying flow physics and combustion chemistry involved in such flows, which ultimately governs the ignition and subsequent combustion processes thereby dictating the effectiveness of this strategy. In this work, we provide a comprehensive overview of the literature on the interaction between the jets in a multiple-injection event, the resulting mixture, and finally the ignition and combustion dynamics as a function of engine operational parameters including injection duration and dwell. The understanding of the underlying processes is facilitated by a new conceptual model of multiple-injection physics. We conclude by identifying the major remaining research questions that need to be addressed to refine and help achieve a design-level understanding to optimize advanced multiple-injection strategies that can lead to higher engine efficiency and lower emissions.

Introduction

Diesel engines are one among the most efficient energy conversion devices and are widely used in ground transportation and commercial applications owing to their high thermal efficiency and low CO_2 emission. Despite their popularity, the diesel engine suffers from high NO_X and particulate emissions. Particularly with more stringent emission regulation requirements, the soot-NO_X trade-off has been posing a serious and consistent challenge and has continuously garnered ever increasing attention over the years [1, 2].

Numerous advanced in-cylinder pre- and post-combustion and injection strategies in addition to various exhaust after-treatment systems have been extensively researched to overcome the soot-NO_X trade-off limitation of diesel engines. The local combustion temperature and equivalence ratio dictate the formation of NO_X and soot in a diesel engine [3]. In a conventional diesel engine, the combustion process is a high temperature, heterogeneous event that covers both NO_X and soot formation areas in the temperature-equivalence ratio soot-NO_X map (Figure 1, [4]). However, by utilizing EGR in conjunction with new combustion modes such as HCCI, PCCI, LTC etc., that facilitate increased fuel-air mixing and dilution, if the combustion temperature can be sufficiently reduced, both NO_X and soot formation can be avoided [4, 5] as highlighted in Figure 1. Higher dilution by increased EGR rates prolongs the ignition delay thereby enhancing the homogeneity of the air-fuel mixture with longer time available for mixing, leading to lower mixture fraction and potentially reduced local equivalence ratios that in turn minimize soot formation [6]. The use of high EGR rates also allows to significantly reduce the in-cylinder combustion temperature and O_2 concentration, therefore reduce NO_X emissions [7].

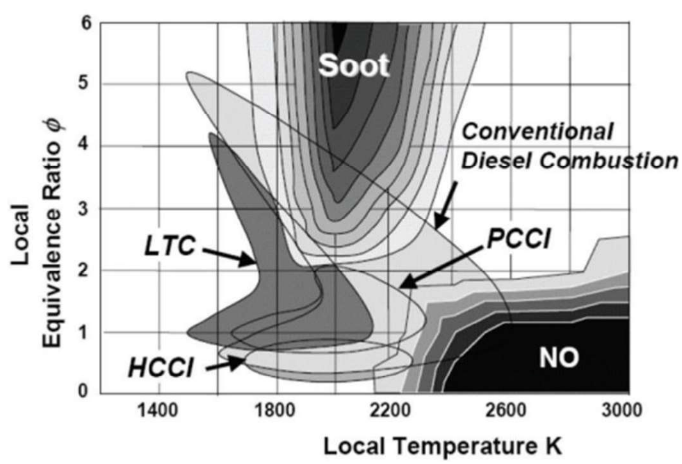

Figure 1. Soot and NO_X formation zones as a function of temperature and equivalence ratio with the conventional and other combustion processes overlaid. Reprinted with permission from [4]. © SAE International.

Multiple-injection and other advanced injection strategies in modern diesel engines

Despite their promise, the implementation of these new in-cylinder combustion modes in production engines continues to face significant limitations, such as combustion control authority, increase in combustion noise and CO/UHC emissions. These limitations usually lead to a restricted use of such modes to lower loads and lower engine speeds [5]. In the case of diesel combustion, among the various solutions proposed to increase this operating envelope, multiple-injection strategies have been widely adopted as this approach has been proven to be effective in reducing combustion noise and in-cylinder NO_X formation while enhancing soot-oxidation [8]. The increased adoption of multiple-injection strategies in modern diesel engines has been mainly attributed to the advent of electronically controlled fuel-injection technologies in conjunction with common-rail direct injection (CRDI). Modern injection technologies are capable of precisely injecting a targeted quantity of fuel more than 8 times per cycle [9], which has allowed for achieving better control over the heat-release and fuel-air mixing processes. Furthermore, advanced injection technologies also provide a higher degree of flexibility in precisely controlling the injection parameters, such as varying injection pressure and number of injections per cycle regardless of engine speed or load conditions without compromising the engine performance and fuel consumption [10].

In a direct-injection diesel engine, a classical (single) injection event consists of a single, uninterrupted, continuous supply of fuel to the combustion chamber. However, in the case of multiple-injections, the fuel is often divided into several smaller quantities, that can be either equal (split injection strategy) or different (early-pilot-post-late injection strategy) in mass and duration as shown in Figure 2. The main difference between these two injection strategies is that in the split injection, the targeted fuel mass is typically distributed uniformly across a pre-determined number of pulses. On the contrary, in a multiple-injection strategy, there is typically a main injection event, which delivers the largest mass of fuel that is preceded (pilot) and / or followed (post) by auxiliary injection pulses capable of injecting a varying quantity of fuel; the same or reduced total injected fuel mass relative to a single injection event is targeted to maintain or even improve the fuel consumption [5].

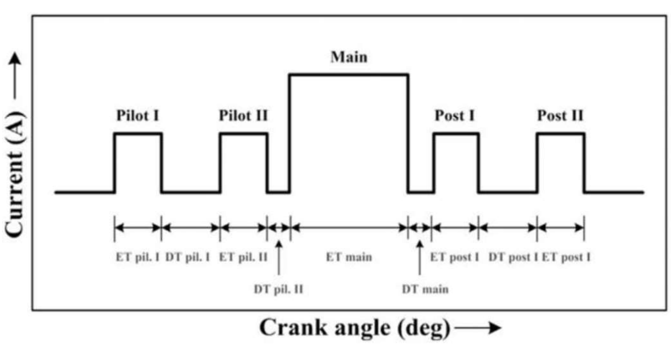

Figure 2. Multiple-injection profile nomenclature. Reprinted from [10], with permission from Elsevier.

The targeted benefits of multiple-injections on engine performance and emissions is summarized in Figure 3. In general, among multiple-injection strategies, split injections are commonly used in HCCI engines to achieve fuel stratification to control the ignition timing and to avoid instantaneous heat release under high-load conditions while reducing the possibility of wall wetting, a potential source for UHC emissions [11]. On the other hand, pilot injections have been shown to decrease the combustion noise of the main injection and NO_X emissions [5, 8, 12-14]; while post injections are more often used for reduction of soot exhaust emissions due to enhanced oxidation [15, 16]. Under conventional engine operation conditions, the pilot injection modifies the conditions in the combustion chamber into which the main injection develops, thereby influencing the combustion performance by decreasing the ignition delay of the main jet [17, 18]. Due to this, the amount of fuel burned in the premixed combustion phase is decreased [5], leading to a reduction of premixed combustion, the associated abrupt heat release, combustion noise and NO_X formation. The exact mechanism of NO_X reduction is unclear as further discussed in the section "NO formation". The post injection tends to introduce momentum in the latter phase of combustion which also enhances mixing within the cylinder bowl and the oxidation of soot formed by the main injection [19, 20]. Furthermore, post injection can also help in managing the exhaust gas temperature for regeneration of diesel particulate filter and to provide hydrocarbons for NO_X adsorber catalyst [21]. Finally, dividing the pilot injection into several smaller injections has been proven effective in further reducing the combustion noise. An alternative/supplemental measure to pilot injection is injection rate shaping, where the injector's internal pressure amplification stages or the needle lift are precisely controlled to reduce the injection rate (and injection pressure) in the initial phase of the main injection, only to ramp up the injection rate in the later stages. This controlled initial rate of injection approach has been shown to further reduce the premixed burn and offers additional NO_X reduction benefits in addition to greatly reducing combustion noise through controlled heat release rates during the premixed and diffusion combustion phases.

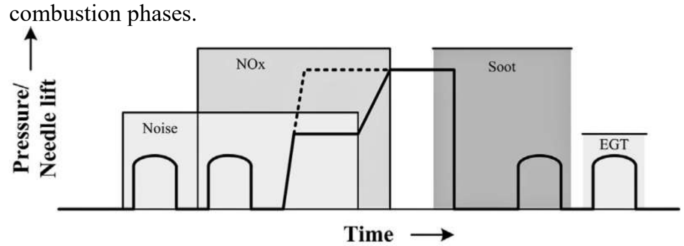

Figure 3. Schematic representation of the different advanced multiple-injection schedules with the corresponding benefit from each injection strategy highlighted. Reprinted from [10], with permission from Elsevier.

The scope of the present review

The physical phenomena involved during multiple-injection process are quite complex as they involve significant interaction between the mixture fields of the two consecutive injections and a strong coupling between the associated ignition and combustion processes; i.e., in a multiple-injection strategy, the resulting combustion process is likely to be a product of the interactions between various injection events. For the purposes of this review we will limit our discussion to a double injection strategy – a first and a second injection. The first injection could be interpreted as either the pilot injection of pilot-main strategy or the first injection of a split injection approach. The same nomenclature is used at a few instances also when an injection schedule resembles a main-post strategy.

While the ignition and the combustion of the first jet is likely to be controlled by the ambient conditions as well as the mixture formation process of itself; the ignition and combustion of the second jet is likely to be influenced by the effects of the first jet in addition to the aforementioned parameters. For example, the combustion or even the low temperature chemistry associated with the first jet would greatly decrease the ignition delay of the second jet [17, 18] under regular engine operating conditions. The flame lift-off length (LOL) of the second jet would be shortened due to the increase of the ambient temperature and/or interactions with the products of the first injection. Furthermore, it is also likely that the combustion products formed from the first injection can quite possibly lead to rapid formation of PAH and soot from the second injection due to a reduced local oxygen concentration [18, 22].

Despite the presence of an extensively documented literature detailing the benefits of multiple-injection on engine performance and emission and its widespread adoption in commercial engines, there is little known about this complex interplay between the underlying flow physics and combustion chemistry involved in such flows. This limited knowledge about the physico-chemical processes that ultimately govern the ignition and subsequent combustion processes in multiple-injection has prevented an efficient and complete optimization of this strategy, thereby limiting its effectiveness. To this end, in this work, we strive to provide a comprehensive overview of the literature on the interaction between the jets in a multiple-injection event, the resulting mixture and finally the ignition and combustion dynamics as a function of engine operational parameters including injection duration and dwell. The focus of this review will be on the underlying governing processes based on studies conducted in optically accessible constant-volume chambers, optical engines, relevant metal engine experiments and numerical studies. This review is not intended to offer an exhaustive view of the engine performance and emission studies involving multiple-injection strategies. Furthermore, we will not be discussing the effect of post-injections on soot-reduction and the associated mechanisms as an extensive review on this aspect was conducted by O'Connor et al [23] and many of the open questions that were then posted have been adequately addressed since then. However, based on past research, a new conceptual model of multiple-injections physics will be presented to outline the existing understanding of underlying processes. We will conclude by identifying the major remaining research questions that need to be addressed to refine and help achieve a design-level understanding to optimize advanced multiple-injection strategies that can lead to higher engine efficiency and lower emissions.

Literature overview of multiple-injection processes in diesel engines

Fuel mixing and jet interaction under non-reactive conditions

Due to the complicated nature of the interaction that exists between the two flow fields in a multiple-injection strategy which governs the mixture formation and ultimately the ignition and combustion of the fuel jets, several researchers have studied this interaction between multiple fuel jets under evaporating, but non-reacting conditions. The experimental studies [17, 24-29] carried out primarily in constant volume chambers heavily relied on high-speed diagnostic techniques such as diffused back illumination (DBI), schlieren imaging [24], laser absorption scattering (LAS) [25-27], and laser induced exciplex fluorescence (LIEF) [28].

The liquid phase [30, 31] and vapor phase penetration [32-34] characteristics of a single injection event are well understood and can be summarized as follows: The liquid length decreases with increasing ambient temperature (faster vaporization), increasing ambient density (more entrainment from a wider spreading angle and increased mass of entrainment per unit volume of the jet at given spatial location) and is approximately independent of fuel-injection pressure. The vapor penetration rate increases with increasing injection pressure (higher initial momentum) and decreasing ambient density (spray narrows, loses momentum slower due to different momentum exchange with lower mass entrainment at a given spatial location) and is approximately independent of ambient temperature.

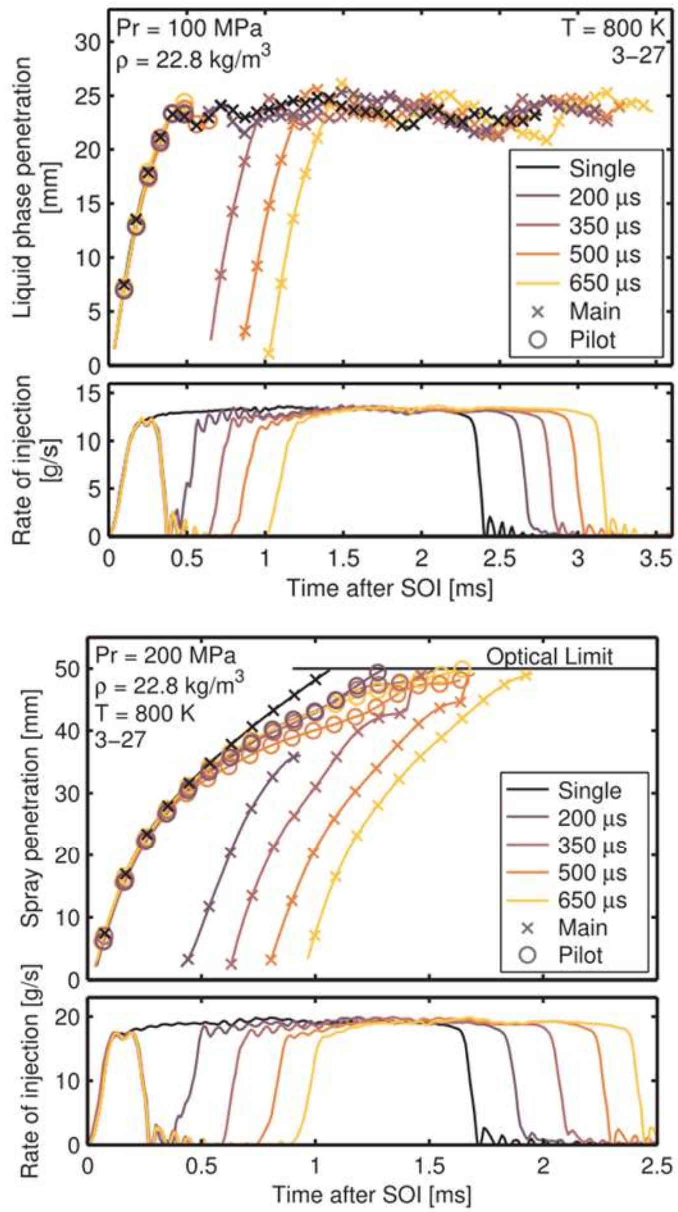

Figure 4. Liquid (top) and vapor (bottom) penetration for a pilot-main multiple-injection strategy with 3mg pilot based on high-speed schlieren imaging. Reprinted from [24], with permission from Elsevier.

The liquid and vapor penetration characteristics in the case of multiple-injection strategy is summarized in Figure 4. In the case of multiple-injections, the stationary liquid length of the second injection is unaffected by both the quantity of fuel contained in the first jet and the hydraulic separation (dwell) between the two injector pulses [24]. However the secondary injection exhibits a higher liquid penetration rate than the prior pulse [24]. Though the rate of penetration of the second injection was higher with decreasing dwell, the liquid phase penetration as well as the liquid phase spreading angle remains fairly constant [24]. The spray penetration rate of the second jet increases with the quantity of fuel contained in the first jet and decreases with increasing the dwell time between the two injections. As the first fuel jet initially accelerates the stationary ambient creating a slipstream [18], the second injection tends to lose less momentum which allows it to penetrate more rapidly [24, 25, 27, 28] resulting in increased mixing at the head of the spray [24, 28]. A shorter dwell time tends to increase this "induced air driving force" as the ambient gases have less time to decelerate i.e., slipstream remains strong. Unlike the liquid phase spreading angle, due to the introduction of the second jet into an ambient with slightly higher density and turbulence levels, some researchers [24] have suggested that the vapor phase spreading angle of the second injection increases. However, this claim about the vapor phase spreading of the second injection has not been universally accepted as other researchers have reported unchanged or reduced spreading angles for the second injection. Despite the possible variation in the spreading angle, the second injection does exhibit a higher rate of penetration [24, 25, 27, 28].

LIEF experiments carried out have shown that the second injection closely follows the contours of the first injection resulting in the same radial extent and same jet angle as indicated by the lack of regions of low fuel concentrations on radial periphery of the second jet [28]. However, more pronounced differences such as a flatter (gradual) fuel concentration gradient at the spray head was observed in the case of multiple-injection. This indicated a strong interaction between the two injections governed by the dwell time, which resulted in increased mixing at the spray head [28]. PIV based velocity measurements have conclusively shown that the degree of interaction between the two fuel jets and the resultant coupling of the flow fields is strongly dependent on the dwell time. At shorter dwell times, the second injection tends to catch up with the first jet and the jets merge to form regions of high velocity at the spray tip that improves the mixture preparation through turbulent mixing [28]. So far, there have been no documented literature studies on reliable and quantitative diagnostic techniques capable of tracking the fuel injections individually i.e., isolate fuel distribution from each injection event in a multiple-injection strategy to help quantify the mixing field between the consecutive injections. Nevertheless, some time resolved mixing field measurements could potentially shed light onto this problem.

The mixture distribution in the liquid and vapor phase at two characteristic times during the main injection for a pilot-main and main-post injection strategy is summarized in Figure 5 and Figure 6 respectively. The amount of air entrained during the injection event is closely linked to the spray length and the spray angle [30, 31, 34, 35]. Thus, for a single injection that is designed to inject the same quantity of fuel as that of multiple-injection strategies, the single injection penetration length is expected to be the longest due to the continuous, uninterrupted flow momentum of the spray lasting for a longer injection duration [25]. The increased penetration length also results in the highest amount of total air-entrainment i.e., leaner fuel-air mixture distribution when compared to multiple-injection strategy. In the case of multiple-injections, due to the change in the ambient concentration caused by the first injection, it is expected that the second injection will entrain fuel-air mixture of reduced oxygen concentration. However in the case of multiple-injections, the "entrainment wave" [36-38] following the end of the first injection will result in rapid leaning out of the air-fuel mixture near the vicinity of the nozzle. Depending on the ratio of fuel contained between the two injections, due to the higher penetration rate of the second injection, it tends to catch up with the first injection [24, 25, 27, 28]. Hence, the mixture formation in the multiple-injection strategy i.e., the local equivalence ratio distribution is highly dependent on the ratio of fuel injected between the two injection pulses [25, 28].

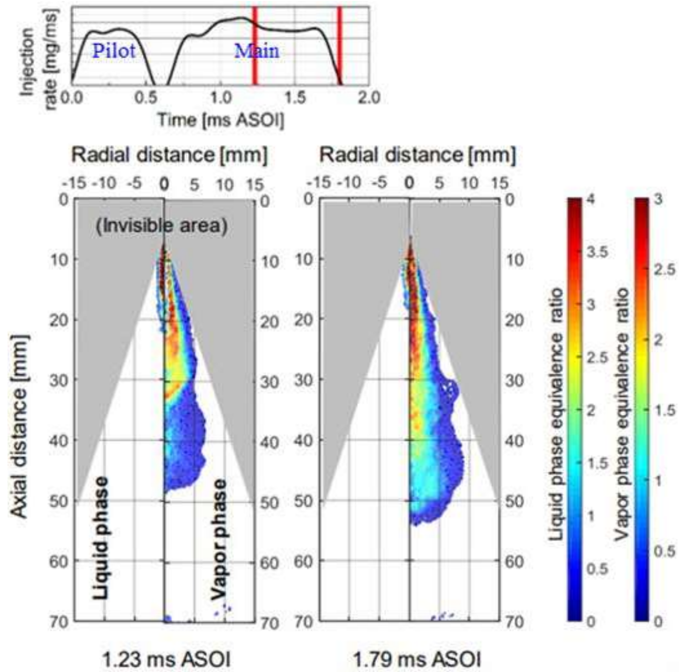

Figure 5. LAS based equivalence ratio evolution in the vapor and liquid phase at two characteristic times during the main injection for a pilot-main injection strategy. Reprinted with permission from [25]. © SAE International.

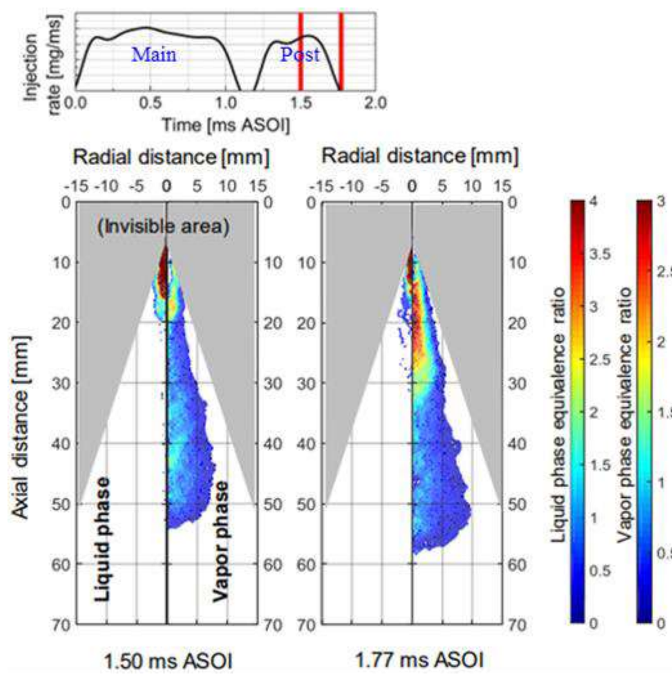

Figure 6. LAS based equivalence ratio evolution in the vapor and liquid phase at two characteristic times during the main injection for a main-post injection strategy. Reprinted with permission from [25]. © SAE International.

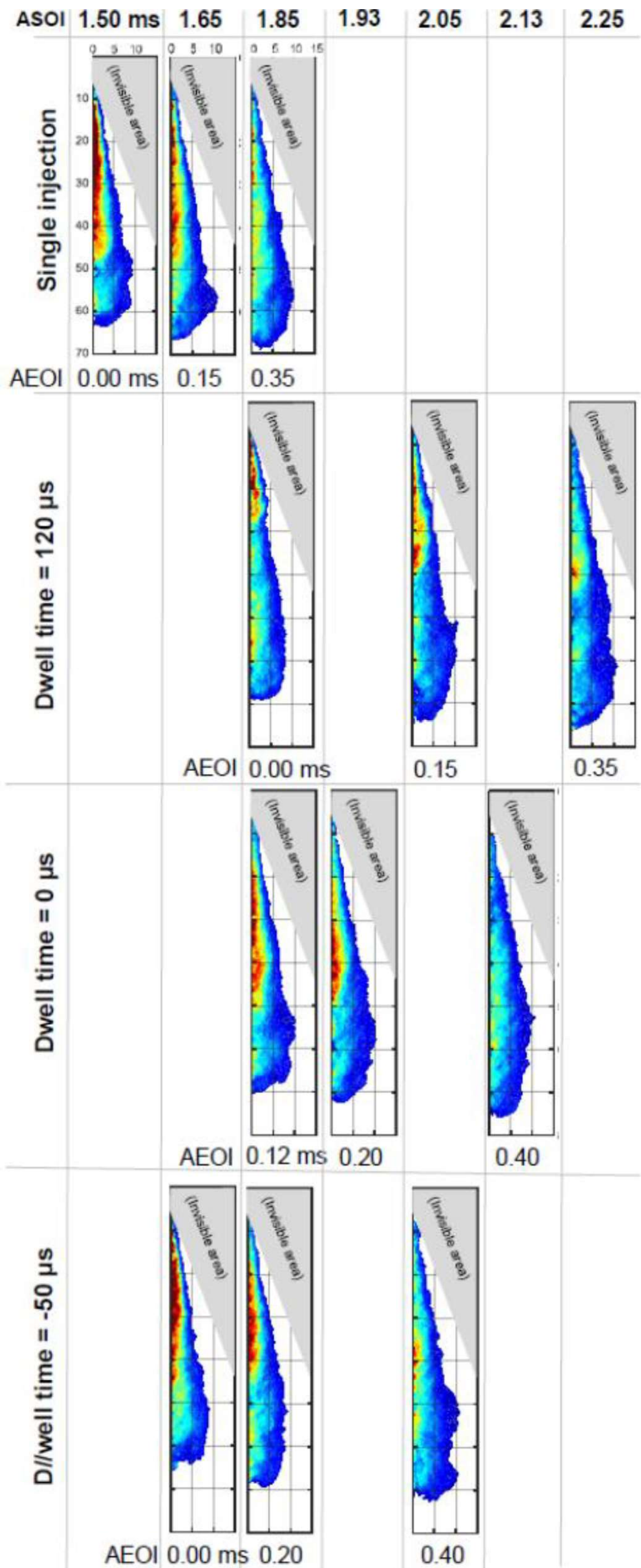

Figure 7. LAS based temporal evolution of the spray mixture formation for various dwell times (negative dwell time indicates a temporary reduction in injection rate though the injection essentially remains a single injection) between the main and post injection schedule. Reprinted with permission from [26]. © SAE International.

In the case of pilot-main strategy (c.f., Figure 5), due to the higher quantity of fuel in the second injection, it tends to quickly catch up with the head of the first injection, resulting in lower overall penetration and thus decreased air entrainment leading to the formation of regions of richer mixtures [25, 28]. In the case of main-post strategy (c.f., Figure 6), due to the reduced quantity of fuel in the second injection, it does not catch up with the head of the first injection, where the entrainment wave from the first injection is still in progress [25, 28]. This favorable positioning of the second jet into the lean regions of the first jet resulted in a more homogenous mixture distribution with an overall lean mixture i.e., equivalence ratio less than unity, by reducing formation of large areas of rich mixtures.

In terms of the effect of dwell time on mixture formation, under non-reactive ambient conditions, increasing dwell times simply resulted in longer available time for leaning out of the first injected fuel and for formation of much leaner regions near the vicinity of the nozzle where the second injection would follow [25, 28]. The temporal evolution of mixture distribution in the vapor phase for a single injection and multiple-injection strategy across various dwell times is summarized in Figure 7. It is to be noted that the negative dwell time corresponds to injections with a temporary reduction in injection rate during the duration of injection, though the injection essentially remains a single injection. The single injection exhibits a more homogenous mixture distribution than the split injection strategy in the ASOI domain as the single injection ends earlier than the multiple-injection strategy. However, the leaning effect of end of injection entrainment wave [36-38] and the slipstream effect [18] is more evident while comparing the injection strategies using the AEOI domain. In this domain, after the end of injection, the split injection strategy with a positive dwell exhibits much smaller regions of richer fuel-air mixture pockets than the single injection. In the case of zero dwell, the small differences observed at the end of injection are soon washed out resulting in a mixture distribution almost equivalent to the positive dwell case. However, in the case of negative dwell, due to a combination of the reduced momentum of the first fuel jet at the end of first injection and the increased momentum of the second fuel jet at the start of the second injection, the second jet catches up with first jet resulting in an overlap of the two spray heads leading to somewhat larger zones of richer mixtures when compared to single injection.

RANS and LES simulations [39-43] on multiple-injection strategies have also independently confirmed the aforementioned experimental findings and provided some valuable additional insights. Due to the "history effect" of the first injection, the second injection exhibits a faster penetration rate thereby increasing the turbulence intensity of the main injection and the associated scalar dissipation rate resulting in enhanced mixing [39-43]. The level of interaction is primarily governed by the dwell time between the two injections and to some extent by the duration and the momentum of the second injection. Though a short post injection following the main injection may not be able to directly influence the mixing process despite a relatively short dwell, it can help mitigate the expedited leaning out of the fuel-air mixture caused by the end of injection entrainment wave by either enriching the fuel-lean regions near the nozzle (low momentum post injection) or by pushing the near-nozzle gases farther downstream where there is enhanced mixing (high momentum post injection). However, under combusting conditions where the combustion products of the first injection are expected to influence the ignition and combustion characteristics of the second injection, the dynamics of mixture distribution and its impact on combustion efficiency in terms of soot and UHC emissions needs to be explored further as net soot generation will be determined by the balance between soot formation and soot oxidation [16, 23].

Some important aspects of modeling multiple-injection strategies in the RANS framework have been revealed in [42]. The RANS models potentially cannot accurately predict the second jet penetration due to the changed in-cylinder flow and turbulence field induced by the first injection, despite their accurate predictions for the single injection cases. It has been shown that re-tuning of the turbulence model parameters might be necessary to accurately capture the second injection. It is unclear whether this limitation universally applies to all simulations in RANS framework. The simulations in LES framework did not experience such drawbacks. An extensive evaluation of CFD simulations' capability to predict mixture distribution in multiple-injections is still lacking; the lack of quantitative mixing data from high-fidelity experiments is a likely contributing factor to this knowledge gap.

Ignition and combustion evolution processes

As discussed earlier, due to the strong interaction between the flow fields of the two injection events, under reactive conditions this interaction is expected to greatly influence the ignition process and the subsequent combustion and resulting pollutant formation. Hence, in the case of multiple-injections, it is justifiable to expect that both the injection strategy and boundary conditions will have a strong influence on the interacting process. Thus in the case of pilot-main strategy, at fairly long dwell times, it is reasonable to expect that the combustion products of the pilot injection will mix sufficiently well with the in-cylinder ambient, so that the ignition delay at any reasonably high bulk gas temperature before the main injection event is indistinguishable from the single injection case. Under shorter dwell times, the combustion products of the pilot injection may not have mixed well with the surrounding in-cylinder ambient and a locally hot region not reflected in the average bulk gas temperature can potentially lead to a much shorter ignition delay of the main combustion than would be suggested by the average bulk gas temperature.

Furthermore, the progress of reactions within the spatial extent of the first injection is of paramount importance to the mixing, ignition, combustion and the pollutant formation associated with the second injection. The potential scenarios for the combustion progress of the first injection during regular operating condition include: vaporization without any reaction, low-temperature chemistry (i.e., first-stage, cool-flame ignition), high-temperature chemistry (i.e., second-stage ignition) without soot formation or high-temperature fuel-rich chemistry leading to soot formation. However, it is justifiable to expect that the different spatio-temporal regions within the first injection are likely to be undergoing all of the possible reaction stages listed above, which makes the dwell time associated with the multiple-injection strategy a critical parameter [18]. With short dwell time between injections, the second injection has been shown to continue its penetration further beyond the upstream, cool flame remnants from the first injection and it tends to ignite and burn closer to the downstream high temperature combustion products from the first injection [28] resulting in a longer lift-off length [17]. However, with a longer dwell, both the cool flame and high temperature combustion products from the first injection recede closer to the injector, which causes the ignition and combustion of the second injection to happen much closer to the injector resulting in a shorter ignition delay with combustion happening in a more fuel-rich mixture [28].

Several researchers have studied this complex interaction between the reactive flow fields of multiple-injections by experimentally probing the spatio-temporal progression of first-stage, low-temperature ignition and the second-stage, high-temperature ignition. Mapping of formaldehyde distribution using PLIF [18, 28, 44-47] or softening (reduction in contrast due to increase in local temperature) in schlieren imaging [18, 44, 46-50] has been widely used as an indicator of first-stage, low-temperature ignition while tracking of second-stage, high-temperature ignition has been typically done through OH-PLIF imaging [28] or OH* chemiluminescence [45] or natural flame luminosity [17, 18, 45, 50].

Under standard ECN Spray A [51] (900 K, 15% O_2, 22.8 kg/m^3) conditions, the typical progress of ignition and combustion for a single injection has been well characterized and can be summarized as follows: The first-stage, low-temperature (cool-flame) ignition that tends to occur first in fuel-lean equivalence ratios present predominantly at the radial periphery of the spray head on the injector side, rapidly spreads as a volumetric first-stage ignition event throughout the spray, which is then followed by the second-stage, high-temperature ignition [22].

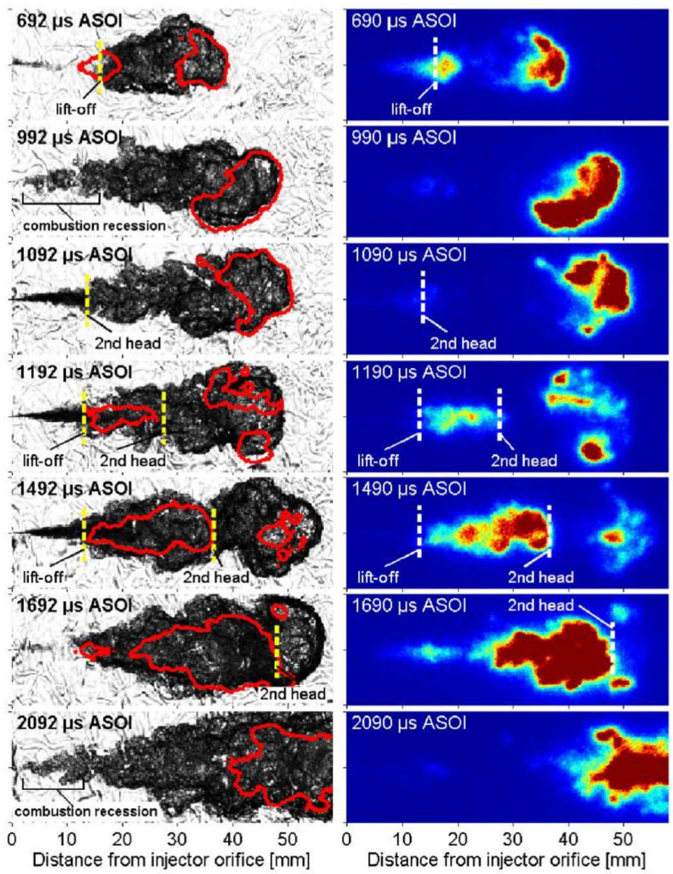

Figure 8. Schlieren (left) and formaldehyde PLIF (right) showing the temporal evolution of ignition as the second jet penetrates into hot burnt residuals from the first injection under 900 K ambient conditions. Reprinted with permission from [18]. © SAE International.

The temporal evolution of the ignition process for multiple-injection strategy under ambient conditions of 900 K and 750 K is summarized in Figure 8 and Figure 9 respectively. At 900 K ambient temperature (c.f. Figure 8), for the first injection, due to its shorter ignition delay (~ 0.17 ms), the formaldehyde that begins to form downstream of the characteristic lift-off length on the injector side [22, 52, 53] is quickly consumed by the progress of "high-temperature combustion recession" [53] whereby, the flame advances from the characteristic lift-off to the near-injector region. Simultaneously increasing amounts of PAH fluorescence is observable at the head of the spray indicating formation of soot precursors [18, 44, 45, 48]. Using a closed homogenous reactor (CHR) formulation based on the estimated adiabatic mixing temperature and the local equivalence ratio using the Musculus-Kattke model [36] near the lift-off length, it has been shown that the second injection penetrates into a high temperature environment (~1200 K) filled with reactive radical species and combustion products from the first injection [18, 28, 44-48]. Due to the rapid penetration of the second injection into this high temperature reactive environment left behind by the first injection, the second injection undergoes rapid progression into second-stage ignition without any evidence of first-stage, cool flame reactions observed earlier for the first injection i.e., the high-temperature ignition delay of the second injection (~0.17 ms) is reduced by a factor of two when compared to the first injection (~0.35 ms) [18, 44-49]. Furthermore, the observed increase in the rate of PAH formation [18, 46, 50] for the second injection is attributed to a combination of the reduced O_2 environment [54] left behind by the first injection and a rapid progression of second-stage combustion with the second injection occurring near the fuel-rich mixtures present around the liquid length. Following the end of the second injection, a second combustion recession follows. It is to be noted that from a practical perspective, the consumption of incomplete combustion products near the injector region following the end of injection can possibly mitigate UHC emissions and improve combustion efficiency.

At 750 K ambient temperature (c.f. Figure 9), due to excessively long ignition delay (~ 2 ms) associated with the first injection, it is still in its cool-flame, first-stage combustion i.e., no onset of second-stage, high temperature combustion as the second injection starts to penetrate. Thus, the second injection now tends to interact with the cool-flame products of the first injection unlike the high temperature

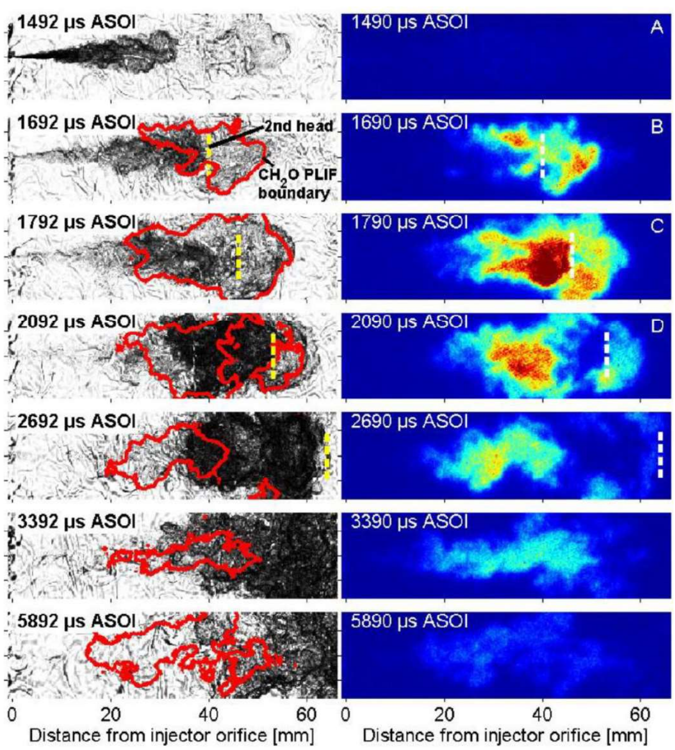

Figure 9. Schlieren (left) and formaldehyde PLIF (right) showing the temporal evolution of ignition as the second jet penetrates into the cool-flame products of the first injection under 750 K ambient conditions. First injection undergoes high-temperature ignition only after interacting with the second injection. Reprinted with permission from [18]. © SAE International.

ambient case discussed earlier [18, 28, 44, 45, 47, 48]. Furthermore, the prolonged ignition delay also allows for a longer mixing time resulting in a moderate, first-stage, heat release resulting in the formation of a more homogeneous fuel-lean mixtures with temperatures close to the 750 K ambient. The interaction of the second injection with the cool-flame products of the first injection leads to its first-stage ignition which is then followed by the onset of second-stage, high-temperature combustion across the entire jet. Although it is unlikely that regions of formaldehyde from the first injection overlap with the spatial extent of the second jet penetration, the observed reduction in the ignition delay of the second injection (again roughly by a factor of 2) can be attributed to the presence of other reactive intermediates such as hydroperoxyl radical that precede formaldehyde formation in cool-flame combustion [18, 44, 46, 48]. Though it was not conclusively shown that the spatial location of the second-stage ignition initiates within the second injection, it is clear that the onset of the second-stage, high temperature ignition is enabled only by the presence of the second injection under these low temperature ambient conditions [18, 44, 47, 48]. Further, as a majority of the upstream and downstream mixture remain fuel lean, high-temperature combustion appears to be confined to isolated regions as indicated by the large regions of formaldehyde signifying broad and persistent zones of incomplete combustion leading to low combustion efficiencies [18, 44]. Despite this, it is important to note that a single injection under similar conditions is unlikely to even undergo second-stage ignition, which would ultimately result in combustion efficiencies far below 75% with increased UHC emissions, making this finding relevant to cold-start and engine idle conditions [18].

RANS [17, 42, 43, 55] and LES [39-42, 46, 56] studies exploring multiple-injection strategies under reactive environments have concurred with the experimental findings discussed earlier, that the dwell time and the boundary conditions have a strong influence on the ignition and combustion processes associated with multiple-injections. Under reactive conditions, the enhanced penetration rate of the second injection is attributed to some extent to the expansion of the burned gas that results in a lower ambient density that reduces the resistance ahead of the second injection in addition to the residual momentum effects from the first injection. In general, based on the dwell time and ambient conditions, there are at least two ways by which that the first injection can change the ignition and combustion characteristics of the second injection resulting in a much shorter ignition delay when compared to the first injection. First, the combustion residuals from the first injection can enhance the reactivity of the near-nozzle region, thereby reducing the ignition delay time of the second injection. Second, the enhanced penetration rate of the second injection causes it to enter the high temperature reaction zone of the first injection, which leads to a reduced ignition delay.

The importance of combustion modeling in the context of split injections was highlighted in [43, 57]. Though simpler combustion models like the popular SAGE model [58] do not account for the turbulence-chemistry interaction, these models are likely to offer a similar performance for modeling multiple injections as when they are used to model single injections. Furthermore, when coupled to a machine learning frameworks, such models have been successfully used to optimize the in-cylinder geometry and the injection strategy with demonstrated performance improvements [59, 60]. However, on the contrary, some more involved combustion models like the CMC [57], RIF [61] and FGM [62] might experience issues when trying to predict the combustion of the second injection. In simpler terms, the progress variable (and/or the local state of the flamelet) results in a memory effect, i.e., when fresh fuel from the second injection enters a computational cell with predominantly burnt products, these models typically predict the fuel rapidly combusting into a fully burnt state, which is in clear contradiction to the experimental observations. Successful extensions to these model have been proposed in an attempt to handle these deficiencies, nevertheless, most commercial codes do not include these extended models in their baseline distributions. Aside from the increased computational cost associated with the use of such advanced models, they also tend to require considerable level of user experience and potentially additional tuning. Furthermore, the sub-grid mixture fraction profile assumptions of these models can be potentially challenged in the case of multiple-injections i.e., in the early stage of interaction between the two jets, the common beta-PDF assumption for sub-grid mixture fraction fails and a bi-modal distribution with the peaks corresponding to the two separate fuel-injection streams was observed particularly in the region where the second jet undergoes ignition [43]. The importance of this finding has not been clarified up to date.

A simulation work in the DNS framework with simplified injection process investigated the interaction process between consecutive injections on a fundamental level [63]. The findings of practical importance include both the sensitivity of ignition delay in the jet interaction zones to local turbulence levels, which can delay the ignition if too high, and the finding that the ignition of the second jet indeed proceeds through autoignition. The presence of burnt products in the air stream tends to delay the ignition, nevertheless, the elevated temperature of the air stream mixed with combustion products prevails and accelerates the ignition.

Formation of NO_X

Several widely accepted chemical pathways have been proposed to describe NO formation. These include: (i) Thermal (Zeldo'vich) mechanism (ii) prompt NO mechanism (iii) Nitrous-oxide (N_2O) mechanism and (iv) Fuel-bound nitrogen conversion to NO mechanism. The thermal NO pathway involves NO formation primarily facilitated through dissociation of molecular nitrogen and oxygen at high gas temperatures. Since the activation energies of the reactions that form NO through the thermal mechanism are relatively high, the chemical equilibrium kinetics that favor formation of NO are fast enough to be significant in engines only at temperatures above 1900 K [64]. The thermal mechanism is most important for stoichiometric and lean premixed flames, and on the oxidizer side of diffusion flames. The prompt NO pathway is initiated when hydrocarbon fragments i.e., CH_X react with atmospheric nitrogen to form intermediate species, such as HCN and NH_X [65]. Depending on the local conditions, these reactive intermediates are either oxidized to form NO, often termed "prompt NO," or react with NO to re-form molecular nitrogen, as in reburning. Prompt NO chemistry is most active in rich premixed flames and on the fuel side of diffusion flames, where there are zones of both significant production and destruction of the intermediate hydrocarbon species [65]. The N_2O mechanism involves NO formation through third-body reactions that lead to the formation of N_2O ($O + N_2 + M$) which on subsequent decomposition yields NO as opposed to the traditional Zeldo'vich direct NO formation pathway. This N_2O pathway plays a significant role in NO formation under lean-premixed environments. In the case of diesel engines, under increased EGR dilution rates that lead to high combustion pressures and lower flame temperatures, N_2O mechanism for NO formation becomes prominent [66]. Since diesel fuels typically contain insignificant quantities (<100 ppm) of fuel-bound nitrogen, the fourth pathway is likely to be unimportant for diesel combustion.

Due to the strong temperature dependency of the NO_X formation kinetics, it is reasonable to expect lower NO_X emissions with reducing reactant and thus reducing adiabatic flame temperature [67]. i.e., NO_X emissions correlate closely to the adiabatic flame temperatures. However, contrary to this widespread understanding, it has also been reported that this expected correlation between NO_X formation and adiabatic flame temperatures does not always hold, especially for operating conditions with large proportions of premixed burn [68]. Under such conditions, it has been reported that combustion phasing alone i.e. compression heating of reactants, is insufficient to explain the observed NO_X trend and the compression heating of burned gases (prior to mixing with cold unburned gases) and the residence time in these environments may be responsible for a part of the observed trend. Under such reduced ambient temperature conditions, the adiabatic flame temperature decreases, but due to the increased ignition delay, the proportion of premixed burn increases. However, the associated equivalence ratio evolution over time i.e. the mass distribution in the equivalence ratio - temperature space with the local peak temperatures being the closer to the adiabatic flame temperature, suggests limited heat dissipation within the volume of burned gases and limited mixing with unburned gases [67]. Due to the high rates of energy release associated with the premixed combustion phase, especially in regions of fuel-rich equivalence ratios, it is possible that combustion products are further compressed by the ongoing reactions that increase the pressure causing their temperatures to increase to super-adiabatic levels (exceeding equilibrium values) briefly resulting in an increased NO_X emissions under premixed burn-dominated operating conditions [68, 69]. But for conditions with excessively long ignition delays, it is expected that part of the premixed fuel is likely to be too lean to form substantial thermal NO_X in the products of premixed burn [68].

Several engine experiments [11, 70-76] have shown that multiple-injection strategies can potentially shift the soot-NO_X trade-off curves of a diesel engine closer to the origin than those operating with conventional single injection thereby reducing both soot and NO_X emissions significantly. Though pilot-main injection strategies have shown to reduce NO_X emissions with only a minimal increase in soot emissions while maintaining the same combustion duration [70-72], the mechanism behind NO_X reduction in the pilot-main strategy is not fully understood. It has been observed that the NO_X exhaust levels depend on the percentage of pilot fuel injected. With increasing quantity of fuel during the pilot injection, there appears to be first a decrease, then a minimum followed by an increase in the measured NO_X levels. The increase in the NO_X levels with continued increase in the pilot fuel quantity is at least in part due to the increase in the average ambient temperature caused by pilot-fuel combustion, despite the resulting decrease in the premixed combustion phase during the main injection event. The pilot-main strategy has been shown to be especially effective under lower load conditions as opposed to medium and high load conditions, where pilot injections have not proved to be effective in achieving NO_X reduction. This is in-line with the understanding that the pilot-injections reduce NO_X formation by limiting the amount of fuel that tends to burn in the premixed combustion phase, which is rather low at high-load conditions with long injections.

One reason for the observed NO_X reduction with multiple-injection strategy is attributed to the ability of the pilot injection to reduce the duration of the main injection thereby allowing its timing to be retarded further compared to the single injection case. The combustion of fuel from the pilot injection increases the ambient temperature and radical concentrations within the cylinder before the start of main injection. This causes a considerable reduction in the ignition delay of the fuel injected during the main injection. Hence, the combustion of the main injection is therefore predominantly mixing controlled and characterized by lower rates of heat release than for premixed combustion. The relatively small amount of pilot fuel, combined with the interruption in the rate of injection, results in a smaller amount of premixed combustion than for a single injection, which on a macroscopic level results on a slower increase of cylinder mean temperature and pressure [8, 13, 14]. Furthermore, the combustion of the pilot injected fuel prior to the main injection can produce a form of internal EGR, i.e., if the quantity of a pilot injection is sufficiently large, the burned gas produced by its combustion will dilute the in-cylinder oxygen concentration for the main injection which also contributes to the reduced NO_X formation. As the Zeldo'vich mechanism is strongly influenced by local temperature and equivalence ratio, the NO formation rate indeed increases with temperature increase and in correspondence of equivalence ratios near stoichiometric conditions. Moreover, the rapid decrease of temperature during the expansion stroke freezes the reactions involving NO_X, causing NO_X exhaust levels greater than those achievable under chemical equilibrium conditions.

One of the remaining questions is the role of prompt NO formation. Some recent advanced optical diagnostics detected substantial NO formation within the diesel jet head, which could be attributed to prompt NO formation [67]. The importance of prompt NO might increase at higher EGR rates (prompt NO formation is not strongly impacted by EGR) as suggested by some numerical simulations of diesel jets [67]. Nevertheless, the formation of prompt NO in diesel jet is still largely unexplored.

In CFD, NO_X models assuming the Zeldovich mechanism in general perform reasonably well and offer some predictive capabilities. Common approaches include either an extension of a chemical mechanism with the extended Zeldovich mechanism or a separate integration of NO_X production using the radical concentrations from either the combustion model or equilibrium radical concentration sub-models [77]. The remaining questions are the importance of prompt NO_X inclusion and the importance of accurately capturing the turbulence-chemistry interactions, which might be challenging considering the model deficiencies discussed in the previous section. At least under certain conditions, the turbulence-chemistry interaction will be important as shown for single injection cases in [67]. NO_X sub-models which modify the local NO_X production rate based on the local scalar dissipation rate could potentially bridge the gap between the direct-integration of combustion models and predictive NO_X modeling under conditions where the turbulence-chemistry interactions can significantly affect the local NO_X production rate. Considering the connection between the premixed-burn phase and the engine-out NO_X discussed earlier, turbulence-chemistry interaction might be of importance for NO_X generation under split injection operation. However, further research is needed to answer these remaining questions.

Preliminary conceptual model of multiple-injection processes: a review of current understanding

Based on the past research, a new conceptual model of multiple-injections physics is presented to outline the existing understanding of the complex interplay between the underlying flow physics and combustion chemistry involved in such flows i.e., the physico-chemical interaction between the multiple-injections, which ultimately govern the ignition and subsequent combustion processes thereby dictating the effectiveness of this strategy.

Mixing

Fuel mixing and penetration of consecutive jets is visualized in Figure 10 based on the existing understanding of multiple-injection interaction, which is limited due to the absence of reliable mixing diagnostics for multiple-injections and only a limited number of published studies. It is clear that the second jet penetrates faster than the first jet, nevertheless, no scaling laws analogous to the scaling laws [34, 35] for a single injection have been published up to date. The second jet penetration is dependent on the dwell time between the injections and likely also on the end-of-injection transients like the steepness of the ROI at the EOI. It was conclusively proven than the liquid length remains constant for both injections despite the faster penetration of the second jet liquid and vapor phase.

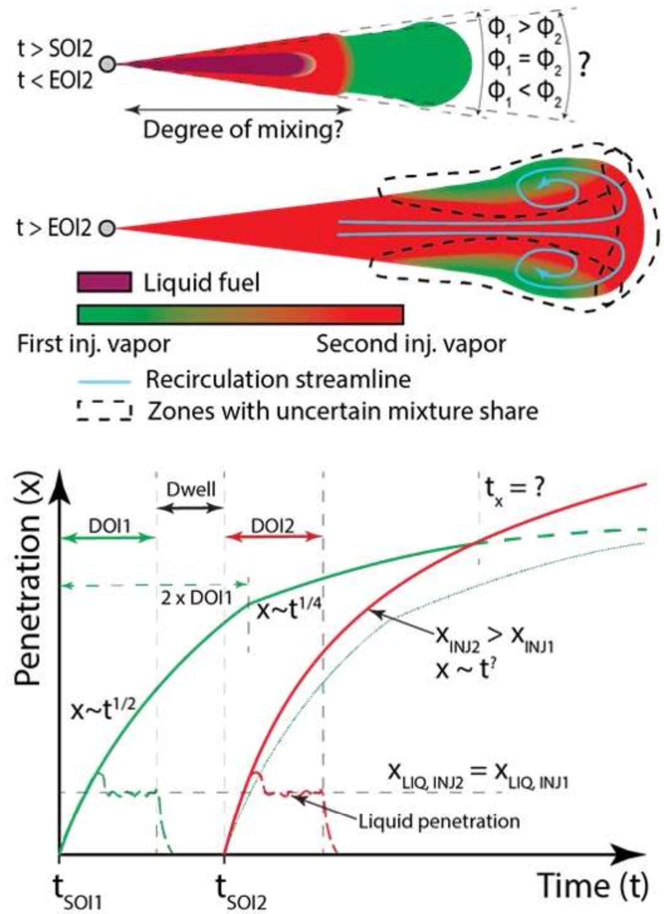

Figure 10. A conceptual schematic of the multiple-injection strategy highlighting the liquid and vapor penetration rates along with the mixture distribution from the first and second injection based on the current understanding. The empirical scaling laws [34, 35] shown here correspond to that of a single injection.

The degree of mixing between the injections and the spreading angle (φ) of the second injection relative to the first injection are contested. The current schematic (c.f. Figure 10) is based on the mixing study from [25, 26, 28] and RANS simulations* investigating the mixing between injections. The spreading angle of the second injection relative to the first injection remains contested, nevertheless, the second injection does catch up with the jet head of the first injection (unless the second injection is very short or the dwell time excessive). RANS simulations showed that the second injection penetrates through the vapor jet of the first injection segregating the first injection fuel vapor to the recirculation zone behind the jet head. Further simulations and/or experiments investigating the mixing between two jets are needed to better characterize the mixing between the jets and the distribution and mixing profile of the jet vapor from each injection.

Fuel ignition and combustion process

The jet-jet interaction, ignition and combustion process strongly depend on the ambient temperature (governing the ignition delay) and the dwell time between injections. Figure 11 visualizes three different scenarios for different ignition delays relative to the injection duration (short, intermediate, long). This conceptual model is primarily based on findings from [18] with further insights from other sources when appropriate/available.

The left column visualizes a short ignition delay case where the first injection undergoes conventional two-stage ignition process (panel 1) and establishes a lifted diffusion flame before the EOI (panel 2). Following the EOI1, the end-of-injection entrainment wave [36] onsets and leads to a lean-out of mixture upstream of the entrainment wave head, limiting the diffusion flame to the jet head (panel 3). At the same time, the flame recesses towards the nozzle resulting in high temperature burnt zones located at short distance from the nozzle orifice. The second injection then penetrates into these hot products of the first injection flame recession (panel 4) and undergoes rapid autoignition. It is unclear whether the second jet undergoes a cool-flame stage or directly transits into high-temperature ignition. The exact mechanism of ignition and the driving mechanisms are not fully known. Following the ignition, a lifted diffusion flame stabilizes with a shorter lift-off distance than observed for the first injection. The mechanism for the shorter lift-off could be increased in-cylinder temperature and/or slow lift-off stabilization following the ignition by hot gases at an upstream location, analogous to the observations when fuel-jet is ignited at an upstream location with a laser spark [78].

The middle column visualizes an intermediate ignition delay scenario with the first jet igniting after the EOI1 but with the ignition delay sufficiently short that the first injection ignites reliably and independently of the second injection progress. In this scenario, the first injection undergoes a cool-flame first stage autoignition either before or after the EOI1. Following the EOI1, the cool-flame recesses towards the nozzle resulting in products of the cool-flame located even very near the nozzle. Depending on the exact conditions, the high temperature autoignition of the first jet occurs near the jet tip, before or somewhat after the SOI2. The prolonged ID1 and therefore, the far-progressed entrainment wave results in a limited extent of the diffusion flame near the jet tip where the equivalence ratio is highest. The high temperature ignition then only slowly recesses towards the nozzle while the second injection penetrates into the cool-flame products of the first injection. The second injection then rapidly experiences cool-flames which are likely accelerated both by the radicals and increased temperature from the first injection cool-flames. High temperature ignition occurs faster than for the first injection and a diffusion flame is established, which encompasses the second injection jet extent downstream of the liftoff length and potentially, the remaining diffusion flame zones from the first injection (panel 4). As the second jet catches up with the first jet penetration, both diffusion flame zones will merge. After the EOI2, the second entrainment wave progresses to reduce the extent of the diffusion flame to the jet tip. The cool flame and the high temperature flame both towards the nozzle, however, due to the lean mixtures near the nozzle the high temperature flame recession stops before reaching the nozzle, leaving regions of UHC near the nozzle regions.

The third scenario (right column, Figure 11) occurs when the charge temperature is very low, resulting in long ignition delay. The first jet might fail to reliably autoignite before a considerable interaction with the second injection occurs. Only the fuel-richest zones within the first injection jet undergo cool-flames leaving extensive zones of unreacted fuel near the nozzle (panel 1). The second injection first penetrates into the unreacted fuel vapor from the first injection (panel 2) before it reaches the cool-flame products (panel 3) and undergoes first stage autoignition earlier relative to the first injection. These cool flame products are at fuel-richer conditions and therefore, proceed to the high-temperature autoignition which is initially limited to the extent of the second injection jet tip (panel 4). The high-temperature flames do slowly spread to leaner mixtures (panel 5) but extensive zones near the edges of the jet and upstream of the burnt flame zones remain too lean to burn or even undergo cool-flames. The diffusion flame might not establish at all since the mixtures potentially lean-out to below stoichiometric before the ignition.

* Personal communication (unpublished data) with Randy Hessel from Wisconsin Engine Research Consultants.

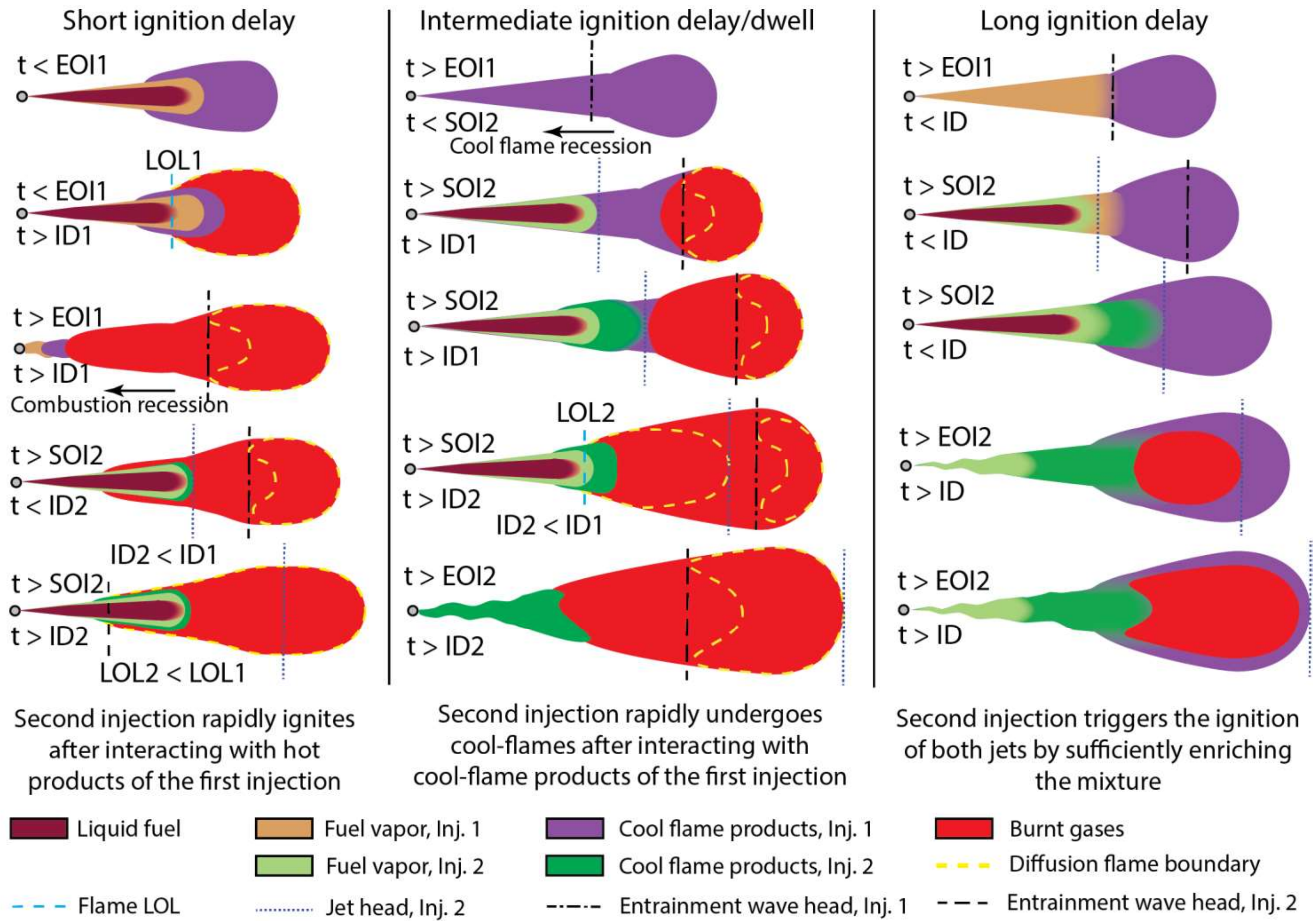

Figure 11. A schematic conceptualizing the ignition and combustion process for two consecutive fuel injections based on the current understanding. Three scenarios depending on the charge temperature (ignition delay) and dwell time are depicted.

Effects of in-cylinder bulk motion, jet-wall and jet-bowl interactions

The jet-jet interactions of free jets under reactive and non-reactive conditions are to some extent understood, however, only very limited literature is available for jets in constrained geometry like the diesel engine combustion chamber. This might be in part due to a large variation of proprietary piston bowl geometries in the commercial products, various approaches regarding the use of swirl and also the differences in the extent of jet-bowl interaction between small-bore light-duty engines and larger heavy-duty and off-road engines. The piston bowl geometry has a strong influence on the in-cylinder air motion as it tends to dictate to a great extent, the development of the complex turbulent flow field at the end of the compression stroke [79]. For example, a wave-shaped piston [80-83] was been shown to improve late-cycle, air-fuel mixing during the diffusion combustion phase by efficiently guiding the near-wall jet flow back towards the combustion chamber center thereby creating a unique recirculation flow known as the radial mixing zone [82]. This radial mixing zone formed by the cylinder flow interactions of the adjacent flames from the fuel jets leads to increased level of turbulence in the reaction layer that improves fuel-air mixing and promotes faster and more complete combustion thereby increasing thermal efficiency and thus reducing soot emissions [80-83].

It is conceivable that the jet impingement on the bowl redirects the gases back towards the center resulting in a 3-dimensional motion which will largely depend on the angle of impingement, jet-jet separation in multi-hole injector and other features in the piston bowl. Experimental studies [84] carried out in constant volume chambers have conclusively shown that soot levels are significantly lower in a plane wall jet (wall impingement) compared to a free jet, most likely caused by the increased fuel-air mixing and a wall-jet-cooling effect. However, jet confinement (simulating jet-jet or jet-adjacent wall interactions) causes combustion gases to be redirected towards the incoming jet, causing the lift-off length to shorten resulting in increased soot generation. However, this effect can be avoided by ending fuel injection prior to the time of significant interaction with redirected combustion gases or by increasing the ambient gas density that delays jet interaction, or by using reduced ambient oxygen concentration that increases the ignition delay [84]. Figure 12 visualizes two potential scenarios of fuel distribution after the first injection impinged on the piston bowl, aiming to demonstrate the implications of different in-cylinder fuel distribution of the progress of subsequent injections. In a scenario with weak recirculation and weak in-cylinder bulk flow (left panel), the jets impinge on the wall but do not create strong recirculation zones and only weakly interact with other jets. This scenario was reported in LTC combustion strategies in

heavy-duty diesel engines [7, 23]. In the case of multiple-injections, in this scenario the ignition and combustion process of the second injection will likely progress analogously to the free jet process (c.f. Figure 12).
A scenario with strong recirculation (and/or strong bulk motion) is depicted on right panel in Figure 12 and results in a distorted first jet fuel distribution relative to a free jet and low-recirculation scenarios. Following the impingement, the jets are redirected in a tangential direction until they interact with the neighboring jets creating zones with the highest fuel concentration in the region between the initial jets. The end-of-injection entrainment rapidly reduces the equivalence ratio on the jet axis. A further distortion of this fuel distribution pattern is possible due to the in-cylinder swirl. When the second jet is initiated it might take longer until it interacts with the first jet fuel or burnt zones. Also, it is possible that the initial jet-jet interaction first occurs at the radial periphery of the second jet rather than at the spray tip. The implications of such a scenario on both the effectiveness of the pilot injection on reducing the ignition delay and NO_X formation and on the needed amount of pilot fuel are currently unclear.

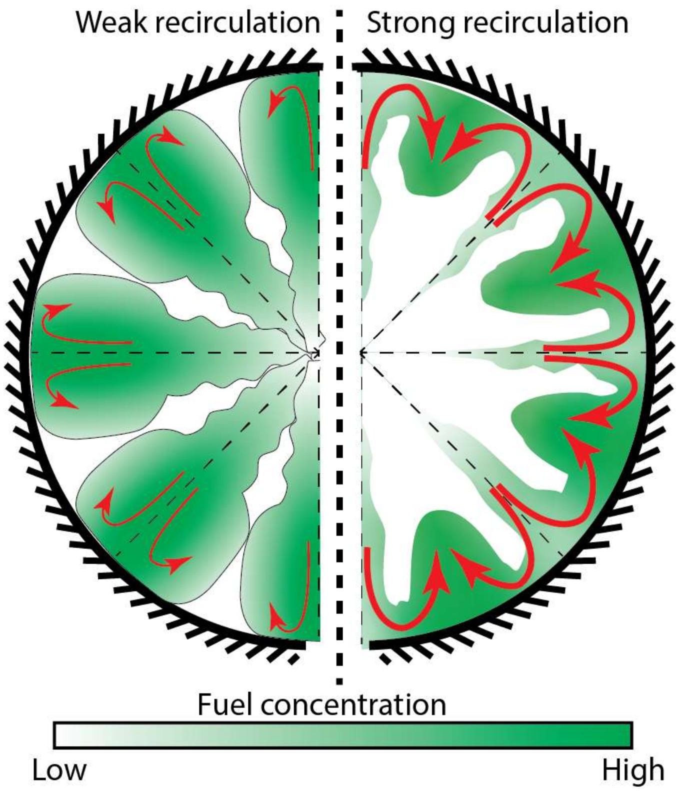

Figure 12. A schematic of potential mixing a fuel distribution scenario in a realistic diesel engine combustion chamber, depending on the strength of recirculation and bulk flow motion.

Summary and Remaining research questions

In summary, many unanswered questions remain a barrier to a design-level understanding of processes governing the interaction between consecutive fuel injections and the resulting mixture, ignition, combustion and pollutant formation processes. This is in part due only a limited body of literature covering this topic with advanced optical methods and high-fidelity simulations, and in part due to the experimental challenges when attempting to distinguish fuel vapor from each injection, accurately visualizing the rapid progress of ignition process in the presence of soot and PAH interferences as well as challenges associated with in-situ visualization of NO_X formation. Since multiple-injections are routinely used in the industry with even more than 8 injections per cycle and the associated multitude of degrees of freedom, improving the understanding of underlying processes can considerably reduce the time and effort needed to develop engine operating maps and highlight the potential technology advances through targeted improvements to the remaining technical challenges. Below, a summary of most prominent remaining research questions is listed:

Mixing

A conceptual understanding of mixing between the jets following the initial interaction is lacking. This is primarily associated with the experimental challenges characterizing such processes and might be resolved by advanced optical techniques or recent advancements in time-resolved mixing diagnostics which might be able to compensate for the lacking specificity regarding which injection the fuel originated from with high temporal resolution allowing to track the features from each injection in time.

Regarding the engineering models of mixing and jet evolution, currently no simple power-laws exist which would describe the second jet cone angle and penetration speed relative to the injection pressure, dwell time and the steepness of SOI and EOI transients.

The other remaining questions are associated with the jet-wall and jet-bowl interactions in realistic combustion chamber geometries. The existing optical engine data provides insights into single-injection mixing processes under non-reactive conditions, nevertheless, the design-level understanding of how the piston-bowl can be optimized to ensure optimal pilot- and post-injection effectiveness remains to be established. Despite the large variation in proprietary piston bowl geometries on the market, such understanding could significantly accelerate the development of new geometries.

Ignition

The remaining questions on the topic of ignition primarily persist on finer details while the general understanding of the interaction of second jet with the first injection has been established. On a more fundamental level, the mechanism of ignition of the second jet under all relevant conditions is not fully understood. The role of flame propagation from an existing diffusion flame, autoignition due to mixing with hot products, radicals from first and second stage ignition and the relative role of each of those should be explored.

A large group of unanswered questions remains regarding the role of EOI transients (steepness of the ROI at EOI, nozzle dribbling, etc.) on the second injection autoignition process. Both the cool-flame and the high-temperature combustion recession will be impacted by the strength of the EOI entrainment wave while the needle dribble might seed large droplet of fuel near the nozzle which can later serve as ignition spots very near the nozzle. The strength of these effects on combustion recession needs to be quantified and it has to be established how each of these processes affect the effectiveness of pilot injection to reduce the ignition delay while potentially avoiding excessive soot production due to fuel ignition at very short axial distances.

Further questions involve the role of piston bowl and bulk cylinder motion on the pilot-fuel ignition, the interaction between the jets and the effectiveness of pilot-fuel injection.

- Recirculation after the first jet impacts the piston bowl – does this intensify or reduce the interaction between the consecutive injections?
- The role of swirl in engines – does swirl reduce the interaction between the jets, and is this desirable or detrimental for the ignition process?
- Can the high turbulence and cold environment in early jets extinguish the recessed flame, only to undergo autoignition at a later time?

NO_X Formation

- The mechanism by which pilot injections can help reduce the NO_X formation – Is it due to reduction of prompt NO_X as result of higher extent of diffusion flame, or differences in associated turbulence-chemistry interactions (lower peak temperature due to turbulent mixing), compression of burnt gases or other mechanisms?
- The role of EGR and effectiveness of pilot injections for NO_X reduction in conjunction with EGR? Does the prompt NO_X take over (higher the EGR, more prompt NO_X is expected)?

References

1. Lu, Y. and Y. Liu, *Effects of multiple injections on combustion and emissions in a heavy-duty diesel engine at high load and low speed.* Advances in Mechanical Engineering, 2020. **12**(12).
2. Mohankumar, S. and P. Senthilkumar, *Particulate matter formation and its control methodologies for diesel engine: A comprehensive review.* Renewable and Sustainable Energy Reviews, 2017. **80**: p. 1227-1238.
3. Kamimoto, T. and M.-h. Bae, *High Combustion Temperature for the Reduction of Particulate in Diesel Engines.* SAE Technical Paper, 880423, 1988.
4. Neely, G.D., et al., *New Diesel Emission Control Strategy to Meet US Tier 2 Emissions Regulations.* SAE Technical Paper, 2005-01-1091, 2005.
5. Mendez, S. and B. Thirouard, *Using Multiple Injection Strategies in Diesel Combustion: Potential to Improve Emissions, Noise and Fuel Economy Trade-Off in Low CR Engines.* SAE International Journal of Fuels and Lubricants, 2008. **1**(1): p. 662-674.
6. Hultqvist, A., et al., *A Study of the Homogeneous Charge Compression Ignition Combustion Process by Chemiluminescence Imaging.* SAE Technical Paper, 1999-01-3680, 1999.
7. Musculus, M.P.B., P.C. Miles, and L.M. Pickett, *Conceptual models for partially premixed low-temperature diesel combustion.* Progress in Energy and Combustion Science, 2013. **39**(2): p. 246-283.
8. Busch, S., K. Zha, and P.C. Miles, *Investigations of closely coupled pilot and main injections as a means to reduce combustion noise in a small-bore direct injection Diesel engine.* International Journal of Engine Research, 2015. **16**(1): p. 13-22.
9. Schöppe, D., et al., *Servo-Driven Piezo Common Rail Diesel Injection System.* ATZautotechnology, 2012. **12**(2): p. 42-47.
10. Mohan, B., W. Yang, and S.k. Chou, *Fuel injection strategies for performance improvement and emissions reduction in compression ignition engines—A review.* Renewable and Sustainable Energy Reviews, 2013. **28**: p. 664-676.
11. Zheng, M. and R. Kumar, *Implementation of multiple-pulse injection strategies to enhance the homogeneity for simultaneous low-NOx and -soot diesel combustion.* International Journal of Thermal Sciences, 2009. **48**(9): p. 1829-1841.
12. d'Ambrosio, S. and A. Ferrari, *Potential of double pilot injection strategies optimized with the design of experiments procedure to improve diesel engine emissions and performance.* Applied Energy, 2015. **155**: p. 918-932.
13. Carlucci, P., A. Ficarella, and D. Laforgia, *Effects on combustion and emissions of early and pilot fuel injections in diesel engines.* International Journal of Engine Research, 2005. **6**(1): p. 43-60.
14. Carlucci, P., A. Ficarella, and D. Laforgia, *Effects of Pilot Injection Parameters on Combustion for Common Rail Diesel Engines.* SAE Technical Paper, 2003-01-0700, 2003.
15. Benajes, J., et al., *Swirl ratio and post injection strategies to improve late cycle diffusion combustion in a light-duty diesel engine.* Applied Thermal Engineering, 2017. **123**: p. 365-376.
16. O'Connor, J., M.P.B. Musculus, and L.M. Pickett, *Effect of post injections on mixture preparation and unburned hydrocarbon emissions in a heavy-duty diesel engine.* Combustion and Flame, 2016. **170**: p. 111-123.
17. Cung, K., et al., *Spray–combustion interaction mechanism of multiple-injection under diesel engine conditions.* Proceedings of the Combustion Institute, 2015. **35**(3): p. 3061-3068.
18. Skeen, S., J. Manin, and L.M. Pickett, *Visualization of Ignition Processes in High-Pressure Sprays with Multiple Injections of n-Dodecane.* SAE International Journal of Engines, 2015. **8**(2): p. 696-715.
19. Mancaruso, E., S.S. Merola, and B.M. Vaglieco, *Study of the multi-injection combustion process in a transparent direct injection common rail diesel engine by means of optical techniques.* International Journal of Engine Research, 2008. **9**(6): p. 483-498.
20. Neel, W., M. Bobba, and M. Musculus, *Effect of Post Injections on In-Cylinder and Exhaust Soot for Low-Temperature Combustion in a Heavy-Duty Diesel Engine.* SAE International Journal of Engines, 2010. **3**(1): p. 496-516.
21. Benajes, J., et al., *Influence of injection conditions and exhaust gas recirculation in a high-speed direct-injection diesel engine operating with a late split injection.* Proceedings of the Institution of Mechanical Engineers, Part D: Journal of Automobile Engineering, 2008. **222**(4): p. 629-641.
22. Skeen, S.A., J. Manin, and L.M. Pickett, *Simultaneous formaldehyde PLIF and high-speed schlieren imaging for ignition visualization in high-pressure spray flames.* Proceedings of the Combustion Institute, 2015. **35**(3): p. 3167-3174.
23. O'Connor, J. and M. Musculus, *Post injections for soot reduction in diesel engines: a review of current understanding.* SAE International Journal of Engines, 2013. **6**(1): p. 400-421.
24. Payri, R., et al., *Study of evaporative diesel spray interaction in multiple injections using optical diagnostics.* Applied Thermal Engineering, 2020. **176**: p. 115402.
25. Kim, J., et al., *Effects of ratio and dwell of split injection on fuel spray and mixture formation process under evaporating, non-reacting condition.* SAE Technical Paper, 2019-01-2323, 2019.
26. Kim, J., et al., *Effects of positive or negative dwell times of split injection on diesel spray development and mixture formation processes.* SAE Technical Paper, 2019-32-0596, 2020.
27. Yang, K., et al., *Characteristics of fuel evaporation, mixture formation and combustion of 2D cavity impinging spray under high-pressure split injection.* Fuel, 2018. **234**: p. 746-756.
28. Bruneaux, G. and D. Maligne, *Study of the mixing and combustion processes of consecutive short double diesel injections.* SAE international journal of engines, 2009. **2**(1): p. 1151-1169.
29. Avinash, G.R.S., et al., *Study of diesel fuel multiple injection characteristics using shadow-graphic imaging technique with*

CRDI system in constant volume chamber. Fuel, 2020. **279**: p. 118436.
30. Siebers, D.L., *Liquid-Phase Fuel Penetration in Diesel Sprays.* SAE Technical Paper, 980809, 1998.
31. Siebers, D.L., *Scaling Liquid-Phase Fuel Penetration in Diesel Sprays Based on Mixing-Limited Vaporization.* SAE Technical Paper, 1999-01-0528, 1999.
32. Payri, R., et al., *Study of liquid and vapor phase behavior on Diesel sprays for heavy duty engine nozzles.* Applied Thermal Engineering, 2016. **107**: p. 365-378.
33. Payri, R., et al., *Differences between single and double-pass schlieren imaging on diesel vapor spray characteristics.* Applied Thermal Engineering, 2017. **125**: p. 220-231.
34. Genzale, C.L., et al., *Relationship Between Diesel Fuel Spray Vapor Penetration/Dispersion and Local Fuel Mixture Fraction.* SAE International Journal of Engines, 2011. **4**(1): p. 764-799.
35. Naber, J.D. and D.L. Siebers, *Effects of Gas Density and Vaporization on Penetration and Dispersion of Diesel Sprays.* SAE Technical Paper, 960034, 1996.
36. Musculus, M.P.B. and K. Kattke, *Entrainment Waves in Diesel Jets.* SAE International Journal of Engines, 2009. **2**(1): p. 1170-1193.
37. Musculus, M.P.B., et al., *End-of-Injection Over-Mixing and Unburned Hydrocarbon Emissions in Low-Temperature-Combustion Diesel Engines.* SAE Technical Paper, 2007-01-0907, 2007.
38. Kook, S., L.M. Pickett, and M.P.B. Musculus, *Influence of Diesel Injection Parameters on End-of-Injection Liquid Length Recession.* SAE International Journal of Engines, 2009. **2**(1): p. 1194-1210.
39. Hadadpour, A., M. Jangi, and X.S. Bai, *Jet-jet interaction in multiple injections: A large-eddy simulation study.* Fuel, 2018. **234**: p. 286-295.
40. Zhao, W., et al., *LES study on the interaction between the local flow and flame structure in multi-injection of n-dodecane.* Fuel, 2021. **285**: p. 119214.
41. Hadadpour, A., et al., *The role of a split injection strategy in the mixture formation and combustion of diesel spray: A large-eddy simulation.* Proceedings of the Combustion Institute, 2019. **37**(4): p. 4709-4716.
42. Blomberg, C.K., et al., *Modeling Split Injections of ECN "Spray A" Using a Conditional Moment Closure Combustion Model with RANS and LES.* SAE International Journal of Engines, 2016. **9**(4): p. 2107-2119.
43. Bolla, M., et al., *Modeling combustion under engine combustion network Spray A conditions with multiple injections using the transported probability density function method.* International Journal of Engine Research, 2017. **18**(1-2): p. 6-14.
44. Maes, N., et al. *Simultaneous High-Speed Formaldehyde PLIF and Schlieren Imaging of Multiple Injections From an ECN Spray D Injector*. in *ASME 2020 Internal Combustion Engine Division Fall Technical Conference*. 2020.
45. Maes, N., et al., *Transient Flame Development in a Constant-Volume Vessel Using a Split-Scheme Injection Strategy.* SAE International Journal of Fuels and Lubricants, 2017. **10**(2): p. 318-327.
46. Moiz, A.A., et al., *Study of soot production for double injections of n-dodecane in CI engine-like conditions.* Combustion and Flame, 2016. **173**: p. 123-131.
47. Moiz, A.A., K.D. Cung, and S.-Y. Lee, *Simultaneous Schlieren–PLIF Studies for Ignition and Soot Luminosity Visualization With Close-Coupled High-Pressure Double Injections of n-Dodecane.* Journal of Energy Resources Technology, 2017. **139**(1).
48. Payri, R., et al., *Analysis of the Influence of Diesel Spray Injection on the Ignition and Soot Formation in Multiple Injection Strategy.* Energies, 2020. **13**(13): p. 3505.
49. Desantes, J.M., et al., *Optical study on characteristics of non-reacting and reacting diesel spray with different strategies of split injection.* International Journal of Engine Research, 2019. **20**(6): p. 606-623.
50. Fan, C., K. Nishida, and Y. Ogata, *Visualization of diesel spray and combustion from lateral side of two-dimensional piston cavity in rapid compression and expansion machine, second report: Effects of injection pressure and interval of split injection.* International Journal of Engine Research. **0**(0): p. 1468087421993062.
51. Bruneaux, G., et al., *Comparison of Diesel Spray Combustion in Different High-Temperature, High-Pressure Facilities.* SAE International Journal of Engines, 2010. **3**(2): p. 156-181.
52. Bruneaux, G., *Combustion structure of free and wall-impinging diesel jets by simultaneous laser-induced fluorescence of formaldehyde, poly-aromatic hydrocarbons, and hydroxides.* International Journal of Engine Research, 2008. **9**(3): p. 249-265.
53. Knox, B.W., et al., *Combustion Recession after End of Injection in Diesel Sprays.* SAE International Journal of Engines, 2015. **8**(2): p. 679-695.
54. Idicheria, C.A. and L.M. Pickett, *Soot Formation in Diesel Combustion under High-EGR Conditions.* SAE Technical Paper, 2005-01-3834, 2005.
55. Zhou, Q., et al., *Computational Modeling of Diesel Spray Combustion with Multiple Injections.* SAE International Journal of Advances and Current Practices in Mobility, 2020. **2**(5): p. 2839-2858.
56. Zhao, W., et al., *Flame–spray interaction and combustion features in split-injection spray flames under diesel engine-like conditions.* Combustion and Flame, 2019. **210**: p. 204-221.
57. Frapolli, N., et al., *Simulations of In-Cylinder Processes in a Diesel Engine Operated with Post-Injections Using an Extended CMC Model.* SAE Technical Paper, 2014-01-2571, 2014.
58. Senecal, P.K., et al., *Multi-Dimensional Modeling of Direct-Injection Diesel Spray Liquid Length and Flame Lift-off Length using CFD and Parallel Detailed Chemistry.* SAE Technical Paper, 2003-01-1043, 2003.
59. Moiz, A.A., et al., *A Machine Learning-Genetic Algorithm (ML-GA) Approach for Rapid Optimization Using High-Performance Computing.* SAE International Journal of Commercial Vehicles, 2018. **11**(5): p. 291-306.
60. Probst, D.M., et al. *Optimization and Uncertainty Analysis of a Diesel Engine Operating Point Using CFD*. in *ASME 2016 Internal Combustion Engine Division Fall Technical Conference*. 2016.
61. Felsch, C., et al., *An extended flamelet model for multiple injections in DI Diesel engines.* Proceedings of the Combustion Institute, 2009. **32**(2): p. 2775-2783.
62. Hasse, C. and N. Peters, *Modelling of ignition mechanisms and pollutant formation in direct-injection diesel engines with multiple injections.* International Journal of Engine Research, 2005. **6**(3): p. 231-246.
63. Wen, X., et al., *Investigation of the ignition processes of a multi-injection flame in a Diesel engine environment using the flamelet model.* Proceedings of the Combustion Institute, 2021. **38**(4): p. 5605-5613.
64. Dec, J.E. and R.E. Canaan, *PLIF Imaging of NO Formation in a DI Diesel Engine* SAE Technical Paper, 980147, 1998.
65. Glarborg, P., et al., *Modeling nitrogen chemistry in combustion.* Progress in Energy and Combustion Science, 2018. **67**: p. 31-68.
66. Mellor, A.M., et al., *Skeletal Mechanism for NOx Chemistry in Diesel Engines.* SAE Technical Paper, 981450, 1998.

67. Brückner, C., et al., *NOx emissions in direct injection diesel engines – part 1: Development of a phenomenological NOx model using experiments and three-dimensional computational fluid dynamics.* International Journal of Engine Research, 2018. **19**(3): p. 308-328.
68. Musculus, M.P.B., *On the Correlation between NOx Emissions and the Diesel Premixed Burn.* SAE Technical Paper, 2004-01-1401, 2004.
69. Pickett, L.M., et al., *Evaluation of the equivalence ratio-temperature region of diesel soot precursor formation using a two-stage Lagrangian model.* International Journal of Engine Research, 2006. **7**(5): p. 349-370.
70. Nehmer, D.A. and R.D. Reitz, *Measurement of the Effect of Injection Rate and Split Injections on Diesel Engine Soot and NOx Emissions.* SAE Technical Paper, 940668, 1994.
71. Pierpont, D.A., D.T. Montgomery, and R.D. Reitz, *Reducing Particulate and NOx Using Multiple Injections and EGR in a D.I. Diesel.* SAE Technical Paper, 950217, 1995.
72. Tow, T.C., D.A. Pierpont, and R.D. Reitz, *Reducing Particulate and NOx Emissions by Using Multiple Injections in a Heavy Duty D.I. Diesel Engine.* SAE Technical Paper, 940897, 1994.
73. Han, Z., et al., *Mechanism of Soot and NOx Emission Reduction Using Multiple-injection in a Diesel Engine.* SAE Technical Paper, 960633, 1996.
74. Chen, S.K., B. Yang, and A.M. Mellor, *Multiple Injections with EGR Effects on NOx Emissions for DI Diesel Engines Analyzed Using an Engineering Model.* SAE Technical Paper, 2002-01-2774, 2002.
75. Chen, S.K., *Simultaneous Reduction of NOx and Particulate Emissions by Using Multiple Injections in a Small Diesel Engine.* SAE Technical Paper, 2000-01-3084, 2000.
76. Jiang, X., et al., *Numerical Study on the Effects of Multiple-Injection Coupled with EGR on Combustion and NOx Emissions in a Marine Diesel Engine.* Energy Procedia, 2019. **158**: p. 4429-4434.
77. Warnatz, J., *NOx Formation in High Temperature Processes*. 2001, University of Stuttgart: Germany.
78. Genzale, C.L., et al., *Laser Ignition of Multi-Injection Gasoline Sprays.* SAE Technical Paper, 2011-01-0659, 2011.
79. Ikeya, N., et al., *Effects of Combustion Chamber Geometry on Diesel Combustion.* SAE Technical Paper, 861186, 1986.
80. Eismark, J., et al., *Role of fuel properties and piston shape in influencing soot oxidation in heavy-duty low swirl diesel engine combustion.* Fuel, 2019. **254**: p. 115568.
81. Eismark, J., et al., *Role of Piston Bowl Shape to Enhance Late-Cycle Soot Oxidation in Low-Swirl Diesel Combustion.* SAE International Journal of Engines, 2019. **12**(3): p. 233-249.
82. Cung, K., et al., *Gasoline compression ignition (GCI) combustion of pump-grade gasoline fuel under high compression ratio diesel engine.* Transportation Engineering, 2021. **4**: p. 100066.
83. Zhang, T., et al., *Effects of a wave-shaped piston bowl geometry on the performance of heavy duty Diesel engines fueled with alcohols and biodiesel blends.* Renewable Energy, 2020. **148**: p. 512-522.
84. López, J.J. and L.M. Pickett, *Jet-Wall Interaction Effects on Diesel Combustion and Soot Formation.* SAE Technical Paper, 2005-01-0921, 2005.

Contact Information

Rajavasanth Rajasegar: rrajase@sandia.gov

Ales Srna: asrna@sandia.gov

Acknowledgments

This research was sponsored by the U.S. Department of Energy (DOE) Office of Energy Efficiency and Renewable Energy (EERE). Sandia National Laboratories is a multi-mission laboratory managed and operated by National Technology and Engineering Solutions of Sandia, LLC., a wholly owned subsidiary of Honeywell International, Inc., for the U.S. Department of Energy's National Nuclear Security Administration (NNSA) under contract DE-NA0003525. The authors gratefully acknowledge fruitful discussions with Mark Musculus.

Definitions/Abbreviations

CO_2	Carbon-di-oxide
NO_X	Nitrogen Oxides
NO	Nitric oxide
N_2O	Nitrous oxide
UHC	Unburned Hydrocarbons
PAH	Polycyclic Aromatic Hydrocarbons
HCCI	Homogeneous Charge Compression Ignition
PCCI	Premixed-Charge Compression Ignition
LTC	Low Temperature Combustion
EGR	Exhaust Gas Recirculation
EGT	Exhaust Gas Temperature
CRDI	Common Rail Direct Injection
DBI	Diffused Back Illumination
LAS	Laser Absorption Scattering
LIEF	Laser Induced Exciplex Fluorescence
PLIF	Planar Laser Induced Fluorescence
ROI	Rate of Injection
SOI	Start of Injection
EOI	End of Injection
ASOI	After Start of Injection
AEOI	After End of Injection
φ	Spreading Angle
LOL	Lift-off Length
ID	Ignition Delay
RANS	Reynolds Averaged Navier Stoke
LES	Large Eddy Simulations
CHR	Closed Homogenous Reactor
CMC	Conditional Moment Closure
RIF	Representative Interactive Flame
FGM	Flamelet Generated Manifold